Spatio-temporal cleaning of a femtosecond laser pulse through interaction with counter-propagating filaments in air

Amélie Jarnac, Magali Durand, Aurélien Houard, Yi Liu, Bernard Prade, Martin Richardson, André Mysyrowicz

Author proofs for: Phys. Rev. A **89**, 023844 (2014)

Spatio-temporal cleaning of a femtosecond laser pulse through interaction with counter-propagating filaments in air

A. Jarnac[1], M. Durand[2], A. Houard[1], Y. Liu[1], B. Prade[1], M. Richardson[2], A. Mysyrowicz[1,*]
[1] *Laboratoire d'Optique Appliquée, ENSTA Paristech, Ecole Polytechnique, CNRS, FR-91762 Palaiseau, France*
[2] *Townes Laser Institute, CREOL, University of Central Florida, Orlando, FL 32816, USA*
**Corresponding author: andre.mysyrowicz@ensta-paristech.fr*

We demonstrate spatio-temporal cleaning of a femtosecond laser pulse impinging on two counter propagating filaments in air. The retro-reflected signal has essentially a perfect beam profile. Pre-pulses present in the incident pulse are also efficiently removed. The performance of the 'filament mirror' is explained by a plasma-mediated wave mixing process that can be viewed as a transient 3d hologram.

The propagation of an intense sub-picosecond laser pulse in air, even with an energy of a few mJ, is highly nonlinear. Two effects play a major role to induce these strong optical nonlinearities during propagation. The first is the optical Kerr effect. By inducing a change of the air refractive index, it leads to beam self-focusing. Although weak at first, self-focusing is cumulative on propagation and becomes precipitous after some distance if the pulse initial peak power exceeds a critical value $P_{cr} = 3.72\lambda_0^2/8\pi n_0 n_2$ which varies between 2.8 GW and 12 GW at 800 nm in normal atmosphere, depending upon pulse duration [1]. Here, n_0 is the linear refractive index, n_2 the non linear index coefficient, and λ_0 is the laser wavelength. The second effect is high field ionization. Total beam collapse is prevented by the onset of ionization, a process requiring the simultaneous absorption of a large number of photons in air. The ensuing plasma is responsible for beam defocusing, an effect which clamps the pulse peak intensity to a value $\sim 5 \times 10^{13}\ \mathrm{W/cm^2}$ [2, 3]. The dynamic competition between optical Kerr induced self-focusing and plasma defocusing thus leads to the emergence of an intense contracted pulse propagating over distances exceeding its Rayleigh length. Due to its high intensity, the contracted pulse leaves in its wake a narrow string of under-dense plasma. This highly nonlinear propagation regime is called filamentation [4].

In this letter, we examine experimentally the situation of three femtosecond laser pulses *1*, *2*, *3* crossing in air, two of which (*1* and *2*) are intense and consist of counter-propagating filamentary pulses. The pulse *3* is weaker and is non collinear. In traditional non-linear optics, a configuration of lower intensity counter-propagating beams forms a phase conjugate mirror that retro-reflects a non collinear wave and inverts its spatial phase [5, 6]. In a similar way, we detect a signal in direction opposite to beam *3*. The counter-propagating filaments thus can be viewed as a transient mirror that retro-reflects part of the incoming beam *3*. However in contrast to the usual case of phase conjugation, the retro-reflected beam (*4*) in the present case has a distortion-free profile, irrespective of the initial spatial phase of beam *3*. We also show that precursor light present in beam *3* is efficiently removed in the retro-reflected pulse. To explain our results we consider the interaction of the three beams in the high intensity limit.

This experiment illustrates the difference between traditional and femtosecond nonlinear optics. The high peak intensity of femtosecond laser pulses leads to specific effects such as non-linear propagation and plasma formation [4]. In addition, this experiment shows that two counter-propagating filaments provide a simple scheme to clean femtosecond laser pulses. Such pulses could find applications in ultrafast physics where femtosecond laser pulses with a high quality beam profile, good stability and a high contrast are needed [7-9].

The principle of the experiment is shown in Fig. 1(a). Two ultra-short laser pulses *1*, *2* of equal peak power > 12 GW undergo filamentation in air and then meet from opposite directions along *z*. The formation of a plasma bubble in the interaction zone is verified by the appearance of a bright spot superimposed on the blue filament luminescence tracks from ionized N_2 molecules [10], as shown in Fig. 1(b). A weaker pulse *3* (beam diameter: 2 mm, P_{max} = 2 GW) is focused with an f = 150 mm lens onto the bubble and is time coincident with the filament pulses. Due to the highly nonlinear ionization rate with laser intensity, the size of the plasma shrinks to a small volume. Through luminescence imaging, we measured the shape of this bubble in the presence of the three pulses. It is an ellipsoid of revolution with axis 11 µm along *z* and 30 µm along *x*, *y*. It induces two signal beams *4*, *4'*, one counter-propagating with beam *3*, the other co-propagating and amplifying it. All laser pulses *1*, *2*, *3* with a central wavelength at 800 nm and duration of

85 fs are derived from the same Ti: Sapphire laser. They are contained in the horizontal plane (*y*, *z*) and are polarized along *x*.

Figure 2 shows an example of a beam profile before and after reflection on the filament mirror recorded with a CCD camera. Here, the incident beam *3* propagates perpendicular to the filament paths ($\theta = 90°$) and is intentionally of poor quality, with a pronounced diffraction pattern and two holes in its fluence profile. By contrast, the retro-reflected pulse *4* has essentially a single spatial mode profile (Fig 2(b)). We have verified that other strong initial beam distortions, such as those introduced by masking part of the beam, are also removed. As shown in Fig. 3(a), the filament mirror reflectivity $R = W_4/W_3$ increases with decreasing angle θ between beams *1* and *3*, where W_i is the energy of pulse *i*. Fig. 3(b) shows *R* as a function of the incident filament pulse energy for a $\theta = 90°$ geometry. One notices a fast increase of the reflected signal *4* above 100 µJ when the pulses *1*, *2* start ionizing air until a plateau is reached with a reflectivity of 10 - 20%. We have also measured an amplification of the transmitted energy of pulse *3* in the presence of the filament pulses. The amplified part *4'* is equal to the retro-reflected signal *4*. It shows that laser energy is transferred from the filament pulses *1*, *2* to the signal pulses *4, 4'*.

To discuss these results, we examine the effect of a change of refractive index of air in the presence of the three waves. The superposition of the three waves *1*, *2*, *3* leads to a transient 3-d plasma hologram that encodes the spatial phase profile of the three beams. The phase profile is dominated by the index variation from the plasma. It is of the form:

$$-\Delta n(t) \approx \int_{-\infty}^{t} [I(t')]^N dt', \qquad (1)$$

where

$$I(t') = |E_1(t' - z/c) + E_2(t' + z/c) + E_3(t' - r/c)|^2, \qquad (2)$$

N is the number of effective photons simultaneously absorbed to create the plasma and E_i the complex electric field of wave *i*. For example E_1 has the standard form:

$$E_1\left(t' - \frac{z}{c}\right) = A_1\left(t' - \frac{z}{c}\right) e^{ik_1 z} e^{i\varphi_1(x,y)} e^{-i\omega t'} \quad (3).$$

The holographic volume is simultaneously read by the three waves. We are concerned with the signal diffracted in the direction opposite to wave *3*.

It takes the general form:

$$E_4 = F(t,x,y,z) e^{i\varphi_1} e^{i\varphi_2} e^{-i\varphi_3} e^{-i\vec{k}_3.\vec{r}}\, e^{-i\omega t}, \quad (4)$$

where *F* is a slowly varying amplitude that includes a number of terms that increases rapidly with *N*. It amounts to 40 terms in the case *N* = 5, which applies to a laser pulse at 800 nm [11]. Note that wave *4* carries the phase of the filament waves and the inverted phase of wave *3*. Pursuing the analogy with optical phase conjugation by degenerate four-wave mixing, we identify the main mechanism responsible for the generation of wave *4*. In conventional degenerate four-wave mixing, a pure index grating diffracts part of the counter-propagating beams in direction $\vec{k}_4 = -\vec{k}_3$. In our model, all incident beams contribute to wave *4*. However the major contribution is due to beams *1* and *2*: the plasma grating formed by filament pulse *1*(*2*) and converging pulse *3* scatters part of the second filament pulse *2*(*1*) at Bragg angle into the direction opposite to the incident beam *3* (dashed-dotted lines in Fig. 1(c, d)). Therefore pulse *4* carries the properties of the intense pulses. Now a remarkable property of filamentation is spatial self-cleaning of the contracted beam profile [12-15] which acquires a Townes mode profile [16].We have verified that pulse *4* fits indeed a Townes mode profile (see Fig. 2(d)). An additional effect plays a role in removing phase distortions of beam *3*, namely the small size of the grating that acts as a filtering pinhole.

To confirm this interpretation, we have measured the signal *4* as a function of delay of pulse *2* with respect to pulses *1* and *3* (see Fig. 4(a)). The signal decays within 30 ps [17], because the plasma grating of long lifetime in air can still diffract a delayed pulse *2* [18]. On the other hand, the signal vanishes within 100 fs if pulse *3* is delayed with respect to the filament pulses (see Fig. 4(b)). This is expected since the formation of the plasma grating requires chronological coincidence of the pulse *3* with at least one of the filamentary pulses.

The filament based mirror also displays interesting temporal pulse cleaning properties. The steep initial increase of the reflectivity shown in Fig. 3(b) is responsible for the removal of laser pulse precursors. Indeed the field interference between precursors present in the three pulses does not form a diffracting plasma grating due to their weaker intensities. On the other hand, the saturated reflectivity region above 1 mJ energy reduces shot-to-shot intensity fluctuations of pulse *4*.

We have verified experimentally the temporal cleaning property of the filament mirror, starting with a laser pulse with a marked temporal precursor, obtained by misaligning the compression stage of the laser. Figure 5 gives the time profile of the pulse, (a) before and (b) after reflection by the filament mirror. The time

profile and the temporal phase of the incident pulse *3* and reflected pulse *4* were obtained with a commercial Frequency-Resolved Optical Gating system apparatus (FROG). Figure 5(b) shows that the front pedestal is totally removed after reflection on the filament mirror. The cleaning properties have also been measured over a larger time scale with a third-order cross correlator [19]. As can be seen in Fig. 5(c), pulse precursors are completely removed over the 10^6 dynamic range of the cross correlator in the trace of the reflected pulse *4*.
Laser pulses with high contrast are desirable for studies of their interaction with intact samples. A pre-pulse, even of modest energy content, can pre-ionize a sample and thereby modify the conditions of interaction at the peak of the pulse [20]. Usual cleaning techniques are (i) the use of pinholes which require strict alignment and are subject to damage [21], (ii) the XPW method which is fragile and expensive [22] or (iii) the plasma mirror which requires a fresh sample after each shot [23]. A filament mirror is cheap since it uses air or another gas as a non-linear material, it is not subject to damage and is relatively easy to align.

In conclusion, we have shown that it is possible to convert a short pulse of arbitrary spatial profile into a single spatial mode pulse by reflecting it on a mirror formed by counter-propagating filaments. The mirror enhances the temporal contrast of the pulse by at least three orders of magnitude. Its action has been described in terms of a transient 3-d plasma hologram. This hologram diffracts part of the filaments light in the direction opposite to that of a third incoming femtosecond laser pulse.

Acknowledgments

The authors thank G. Hamoniaux and P. Rousseau for technical help. This work was partially supported by DGA through a Ph. D. grant.

References

[1] J. K. Wahlstrand, Y-H. Cheng, and H. M. Milchberg, Phys. Rev. A **85**, 43820 (2012)
[2] H. R. Lange, A. Chiron, J-F. Ripoche, A. Mysyrowicz, A. Breger, and P. Agostini, Phys. Rev. Lett. **81**, 1611 (1998)
[3] J. Kasparian, R. Sauerbrey, and S. L. Chin, Appl. Phys. B **71**, 877 (2000)
[4] For a review, see A. Couairon,and A. Mysyrowicz, Phys. Rep. **441**, 47 (2007)
[5] R. A. Fisher, Ed., *Optical Phase Conjugation* (Academic Press, New York, 1983)
[6] R. W. Boyd, *Nonlinear Optics* (Academic Press, Amsterdam, 2008), chap. 7
[7] T. Ceccotti, A. Lévy, H. Popescu, F. Réau, P. D'Oliveira, P. Monot, J. P. Geindre, E. Lefebvre, and Ph. Martin, Phys. Rev. Lett. **99**, 185002 (2007)
[8] N. M. Naumova, J. A. Nees, I. V. Sokolov, B. Hou, and G. A. Mourou, Phys. Rev. Lett. **92**, 063902 (2004)
[9] J. A. Wheeler, A. Borot, S. Monchocé, H. Vincenti, A. Ricci, A. Malvache, R. Lopez-Martens, and F. Quéré, Nat. Photon. **6**, 829–833 (2012)
[10] A. Talebpour, S. Petit, and S. L. Chin, Opt. Commun. **171**, 285 (1999)
[11] S. L. Chin, "From Multiphoton to Tunnel Ionization", in: S. H. Lin, A. A. Villaeys, Y. Fujimura (Eds.), Advances in Multiphoton Processes and Spectroscopy, World Scientific, Singapore, **16**, 2004, pp 249-272.
[12] B. Prade, M. Franco, A. Mysyrowicz, A. Couairon, H. Buersing, B. Eberle, M. Krenz, D. Seiffer, and O. Vasseur, Opt. Lett. **31**, 17 (2006)
[13] C. P. Hauri, W. Kornelis, F. W. Helbing, A. Heinrich, A. Couairon, A. Mysyrowicz, J. Biegert, and U. Keller, Appl. Phys. B **79**, 673 (2004)
[14] X. Chen, Y. Leng, J. Liu, Y. Zhu, R. Li, and Z. Xu, Opt. Commun. **259**, 331 (2006)
[15] F. Theberge, N. Akozbek, W. Liu, A. Becker, and S. L. Chin, Phys. Rev. Lett. **97**, 023904 (2006)
[16] K. Moll, A. Gaeta, and G. Fibich, Phys. Rev. Lett. **90**, 203902 (2003)
[17] M. Durand, A. Jarnac, Y. Liu, B. Prade, A. Houard, V. Tikhonchuk, and A. Mysyrowicz, Phys. Rev. E **86**, 036405 (2012)
[18] Note when a short pulse 2 delay δt is introduced, a fringe pattern becomes apparent in the spatial profile of pulse 4, with a fringe separation decreasing with delay. This pattern is due to the formation of a second displaced grating formed by interference of pulse 2 with the edge of pulse 3. It disappears at delays $\delta t > 150$ fs.
[19] A. Jullien, O. Albert, F. Burgy, G. Hamoniaux, J.-P. Rousseau, J.-P. Chambaret, F. Augé-Rochereau, G. Chériaux, J. Etchepare, N. Minkovski and S. M. Saltiel, Opt. Lett. **30**, 920 (2005)

[20] M. Kaluza, J. Schreiber, M. I. K. Santala, G. D. Tsakiris, K. Eidmann, J. Meyer-ter-Vehn, and K. J. Witte, Phys. Rev. Lett. **93**, 045003 (2004)
[21] P. M. Celliers, K. G. Estabrook, R. J. Wallace, J. E. Murray, L. B. Da Silva, B. J. MacGowan, B. M. Van Wonterghem, and K. R. Manes, Appl. Opt. **37**, 2371-2378 (1998)
[22] A. Ricci, A. Jullien, J-P. Rousseau, Y. Liu, A. Houard, P. Ramirez, D. Papadopoulos, A. Pellegrina, P. Georges, F. Druon, N. Forget, and R. Lopez-Martens, Rev. Sci. Instrum. **84**, 043106 (2013)
[23] C. Thaury, F. Quéré, J.-P. Geindre, A. Levy, T. Ceccotti, P. Monot, M. Bougeard, F. Réau, P. d'Oliveira, P. Audebert, R. Marjoribanks, and P. Martin, Nat. Phys. **3**, 424 (2007)

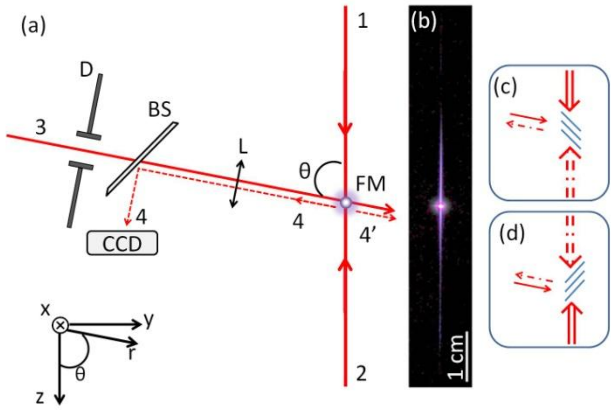

FIG. 1. (a) Schematic set-up. D: diaphragm; BS: beam splitter; L: lens; CCD: charge coupled device camera; FM: filament mirror. (b) Photograph of the blue plasma luminescence emitted by the three overlapping beams; (c) and (d) Schematic diagram of the main diffraction process giving rise to the signal beam *4*.

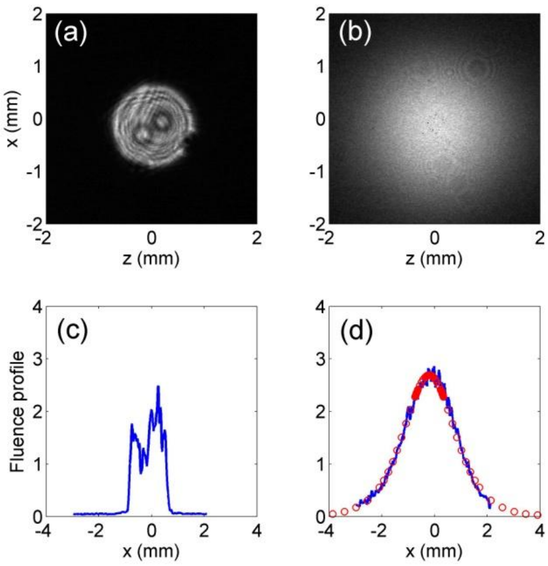

FIG. 2. Fluence profile of a femtosecond pulse before (a) and after (b) reflection on the filament mirror, as recorded in a single shot with a CCD camera. Scan of the fluence profile along x at $z = 0$, before (c) and after (d) reflection. The red open circles represent a fit of the reflected beam *4* by a Townes mode profile function.

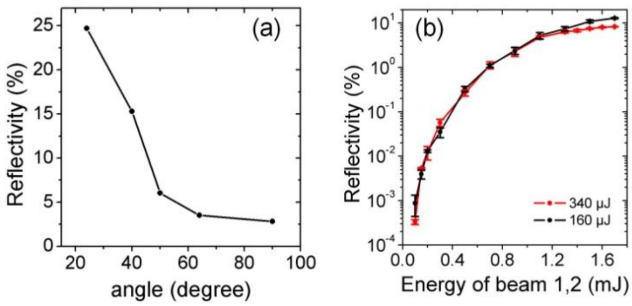

FIG. 3 (a) Reflectivity (R = W_4/W_3) of the filament mirror as a function of angle θ between pulse *1* and *3*. Here W_1 = W_2 = 0.8 mJ; W_3 = 170 µJ. (b) Reflectivity as a function of pulse *1*, *2* energy. Pulse *3* has energy of 160 and 340 µJ and is incident at an angle of 90°. The three pulses are coincident in time.

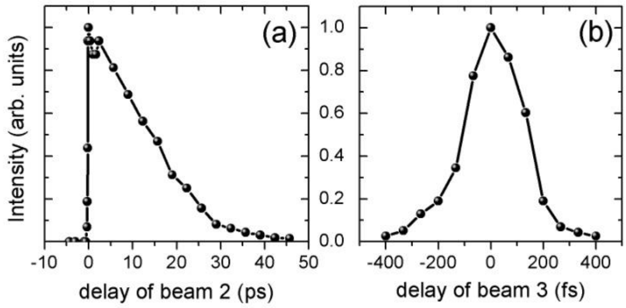

FIG. 4. (a) Signal of pulse *4* as a function of delay of filament pulse *2*. Pulse *3* is incident at an angle of 90°. Pulses *1* and *3* are coincident in time. (b) The same, but delaying the pulse *3* with respect to pulses *1* and *2*.

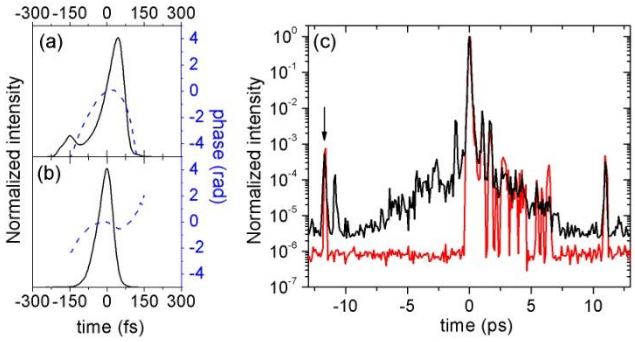

FIG. 5. Temporal profile of incident pulse *3* (a) and reflected pulse *4* (b) measured with a FROG apparatus. (c) Contrast measurement performed with a 3ω cross-correlator of laser pulse *3* before (black line) and after (red line) reflection by the filament mirror. The black arrow indicates an artifact of the correlator.